Title

Distinct patterns of GABAergic interneuron pathology in autism are associated with intellectual impairment and stereotypic behaviors

Journal

Autism, 27(6)

ISSN

1362-3613

Authors

Dufour, Brett D

McBride, Erin

Bartley, Trevor

et al.

Publication Date

2023-08-01

DOI

10.1177/13623613231154053

Peer reviewed

HHS Public Access

Author manuscript

Autism. Author manuscript; available in PMC 2024 February 06.

Published in final edited form as:

Autism. 2023 August ; 27(6): 1730–1745. doi:10.1177/13623613231154053.

Distinct patterns of GABAergic interneuron pathology in autism are associated with intellectual impairment and stereotypic behaviors

Brett D Dufour[1,2,3], **Erin McBride**[2,3,4], **Trevor Bartley**[2,3,4], **Pablo Juarez**[2,3], **Verónica Martínez-Cerdeño**[2,3,4]

[1]UC Davis Department of Psychiatry and Behavioral Sciences, USA

[2]UC Davis School of Medicine, USA

[3]Institute for Pediatric Regenerative Medicine, USA

[4]UC Davis Department of Pathology and Laboratory Medicine, USA

Abstract

Autism spectrum disorder is a neurodevelopmental condition characterized by deficits in social communication and repetitive behaviors. How specific anatomical alterations contribute to the clinical profile of autism spectrum disorder remains largely uncharacterized. We have previously shown that parvalbumin-positive Chandelier cells, a specific type of GABAergic interneuron, are reduced in number in the autism spectrum disorder prefrontal cortex. Here, we assessed the relationship between interneuron pathology with autism spectrum disorder symptom severity and comorbidity. We collected clinical records from autism ($n = 20$) and control ($n = 19$) brain donors, from whom we previously characterized GABAergic interneuron pathology in three regions of the prefrontal cortex (BA9, 46, and 47). We assessed the relationship between the severity of core symptoms, as indicated by Autism Diagnostic Interview—Revised scores, and Chandelier cell pathology in autism spectrum disorder, and also differences in interneuron

Corresponding author: Verónica Martínez-Cerdeño, Institute for Pediatric Regenerative Medicine (IPRM), Shriners Hospitals for Children and UC Davis School of Medicine, 2425 Stockton Boulevard, Sacramento, CA 95817, USA. vmartinezcerdeno@ucdavis.edu.

Authors' contributions

BDD designed experiment, collected/retrieved clinical and pathology data, and performed statistical analysis, imaging, figures, and wrote manuscript. EM extracted and coded clinical data from patient records. TB and PJ helped with staining/imaging. VMC designed experiment, supervised the project, and wrote manuscript.

Ethical approval and consent to participate

All work here utilized de-identified postmortem brain tissue and clinical records obtained from the NIH Neurobiobank and the Autism Tissue Program. De-identified tissue and clinical records have been deemed by the UC Davis Institutional Review Board as "not human research" as the information pertains to deceased donors and no PII is present. Thus, this research was considered exempted from needing IRB review by the UC Davis IRB review board (IRB exemption number 859356-1).

Consent for publication

All data included for publication comes from de-identified brain tissue donors, including both the tissue itself and associated clinical records. Consent for tissue donation and access to clinical records was obtained and is in possession by each brain bank (NIH Neurobiobank and Autism Tissue Program), who carried out de-identification of the data utilized here. The authors do not have access to the donor's name or any PII from the tissue/records, nor can they contact next of kin to obtain further/secondary consent.

Supplemental material

Supplemental material for this article is available online.

Declaration of conflicting interests

The author(s) declared no potential conflicts of interest with respect to the research, authorship, and/or publication of this article.

pathology associated with autism spectrum disorder comorbidities. Total GABAergic interneuron number was significantly reduced in autism spectrum disorder cases with intellectual disability in the prefrontal cortex (PFC)—by 36.6% relative to autism spectrum disorder without intellectual disability and by 38.7% relative to neurotypical controls. The severity of autism spectrum disorder motor stereotypies was correlated with the severity of Chandelier cell loss in BA47, as indicated by reductions in parvalbumin^{+} interneurons and GABA transporter 1^{+} cartridges. Chandelier cell loss is associated with the core autism spectrum disorder symptom domain of restricted repetitive behaviors and likely plays a role in stereotypic motor mannerisms. Intellectual impairment in autism spectrum disorder reflects a more severe form of a common underlying neuropathology-cortical GABAergic interneuron loss.

Lay Abstract

Autism spectrum disorder is a neurodevelopmental condition characterized by deficits in sociability and communication and the presence of repetitive behaviors. How specific pathological alterations of the brain contribute to the clinical profile of autism spectrum disorder remains unknown. We previously found that a specific type of inhibitory interneuron is reduced in number in the autism spectrum disorder prefrontal cortex. Here, we assessed the relationship between interneuron reduction and autism spectrum disorder symptom severity. We collected clinical records from autism spectrum disorder (n = 20) and assessed the relationship between the severity of symptoms and interneuron number. We found that the reduced number of inhibitory interneurons that we previously reported is linked to specific symptoms of autism spectrum disorder, particularly stereotypic movements and intellectual impairments.

Keywords

autism; behavior; human; interneuron; postmortem

Introduction

Autism spectrum disorder (ASD) is a neurodevelopmental disorder characterized by social communication deficits and restricted repetitive patterns of behavior (RRB). Symptoms from both domains and evidence of early onset (<36 months) must be present for diagnosis (American Psychiatric Association, 2013). Social communication deficits manifest as impairments in social-emotional reciprocity, nonverbal communication used for social interaction, and/or developing and maintaining relationships (American Psychiatric Association, 2013). RRBs manifest as circumscribed interests, a compulsive need for sameness, stereotypic motor behaviors, and/or altered reactivity to sensory input (American Psychiatric Association, 2013). Epilepsy (Kohane et al., 2012), intellectual disability (Maenner et al., 2020), and language deficits (Sterponi et al., 2015) are prevalent comorbidities.

We have an incomplete understanding of the pathophysiological mechanisms that underlie ASD. Human postmortem studies indicate that ASD cases show altered brain growth trajectories and increased neuron number (Courchesne et al., 2011; Falcone et al., 2021). Heterotopias and focal dysplasia are common (Wegiel et al., 2010), and likely reflect

abnormalities in prenatal cell proliferation and migration (Wegiel et al., 2010). Cortical minicolumns show disrupted organization and wider spacing (Casanova et al., 2002), and pyramidal neurons show increased dendritic spine density (Hutsler & Zhang, 2010). More recently, we (Amina et al., 2021; Ariza et al., 2018; Hashemi et al., 2017) and other groups (Adorjan et al., 2017; Lawrence et al., 2010) have identified alterations in GABAergic interneurons (INs) in the human postmortem ASD brain. INs are inhibitory neurons that compose 20%–30% of all neocortical neurons, forming a network that regulates the activity of local pyramidal glutamatergic projection neurons and each other (DeFelipe et al., 2013; Hof et al., 1999). Numerous distinct subtypes of INs have been identified based on differences in cell morphology, electrophysiology, and circuit connectivity (DeFelipe et al., 2013; Zaitsev et al., 2005). While there are no specific markers that individually label each subtype, the calcium-binding proteins calretinin (CR), calbindin (CB), and parvalbumin (PV) are frequently used to identify and characterize subpopulations of INs (Hof et al., 1999; Zaitsev et al., 2005). These markers are exclusively expressed by INs in largely a nonoverlapping fashion (Hof et al., 1999; Zaitsev et al., 2005).

Our group first identified a specific ~30%–60% reduction in PV^+ IN number in three regions (BA9, 46, and 47, [Figure 1A])of the ASD prefrontal cortex (Hashemi et al., 2017), while CR^+ and CB^+ IN numbers were not altered (Hashemi et al., 2017). These regions of PFC were of particular interest in the initial study due to their known involvement in ASD-relevant behavioral function—including complex cognitive ability (Snow, 2016), language (Hertrich et al., 2021), behavioral control (Tanji & Hoshi, 2008), and social behavior (Beer et al., 2006). We next demonstrated that this loss of PV^+ INs reflected a specific loss of PV^+ Chandelier cells (ChCs) (Ariza et al., 2018). PV^+ basket cells, the only other PV^+ IN subtype, were not different between ASD and control cases (Ariza et al., 2018). ChCs have a unique morphology, circuit connectivity, and function in the neocortex. These are characterized by large axonal arbors that terminate in a short series of GABA Transporter 1 (GAT1) positive puncta, called cartridges (Figure 1B) (DeFelipe & Gonzalez-Albo, 1998; Wang et al., 2016). ChC cartridges synapse exclusively on the axon initial segment (AIS) of pyramidal neurons, where they regulate action potential generation (Wang et al., 2016). In a third experiment, we identified that $GAT1^+$ cartridges are also reduced by the same percentage as PV^+ INs in the same three regions of the ASD PFC, which corroborates our initial finding of reduced ChCs (Amina et al., 2021).

It remains poorly understood how any known human ASD neuropathology, including our recent findings of alterations of PFC ChCs, is related to specific ASD symptoms. Here, in a retrospective study, we aimed to better understand how our previous findings of IN pathology in the ASD PFC correspond to ASD symptoms and comorbidities. To do so, we acquired detailed clinical records from the brain donors used in previous studies (Amina et al., 2021; Hashemi et al., 2017) and statistically assessed the relationship between ChC loss (data generated previously) and patient clinical profile. While this was an exploratory study based on ASD symptom heterogeneity, it was guided by a broad overarching hypothesis that the severity of specific ASD symptoms corresponds to the pattern and/or severity of IN pathology in the prefrontal cortex.

Methods

Cases and tissue

We obtained formalin-fixed postmortem brain tissue from the NIH Neurobiobank (NBB) and the Autism Tissue Program (ATP), (Table I). ASD diagnosis was confirmed postmortem using the Autism Diagnostic Interview—Revised (ADI-R). The brain bank dissected three blocks of tissue (1 cm × 1 cm × 0.5 cm) from the PFC (BA9, BA 46, and BA 47, [Figure 1A] from each case, and shipped to UC Davis. Blocks were submerged in 30% sucrose, embedded in OCT and frozen, sectioned at 14 μm using a Cyrostat (Leica), and stored at −20 C until staining.

Neuropathology

We used neuropathology data from our previously published IHC studies that identified a reduction in PV^+ neuron number and in ChC cartridge number in the ASD brain (Amina et al., 2021; Hashemi et al., 2017). In these studies, we used triple enzymatic IHC against calbindin (CB-D28k, mouse monoclonal, 1:500, Swant 6797), Calretinin (CR, rabbit polyclonal, 1:500, Swant 7697), and PV (1:500, Swant 235) to stain interneurons (Figure 1C), and single enzymatic IHC against GABA transporter 1 (GAT1, rabbit polyclonal, 1:250, Abcam ab426) to stain ChC cartridges (Figure 1C). The same standard immunohistochemical procedure was used for all sections/stains, which included: incubation in 50% ethanol/chloroform, re-hydration in graded alcohols, heat-mediated antigen retrieval using a Diva decloaker (DV2004 LX, MX, Biocare medical), incubation in 3% H_20_2 for 20 min. to block endogenous peroxidase, incubation in Bloxall Reagent (Vector Laboratories) to block other types of nonspecific staining, incubation in 10% donkey serum to block nonspecific antibody binding, overnight incubation in primary antibody solution (10% serum, .03% Triton, in TBS) at 4 C, 1 h incubation in secondary antibody solution the second day, 1 h incubation in ABC reagent (Vector), followed by visualization with a desired detection kit (Vector DAB, Vector NovaRed, or Vector AP Blue). Tissue was washed three times between each step with TBS/TBS-Tween. After staining, tissue was dehydrated using graded alcohols, cleared in xylenes, and coverslipped using paramount.

Stereoinvestigator software was used for the quantification of INs and cartridges. All cells or cartridges were quantified within a 3-mm wide (horizontally running along the pial surface) counting frame that spanned all cortical layers (vertically). We compared the total number of PV^+ neurons and $GAT1^+$ cartridges, and the ratio between PV^+ neurons to the total number of INs (CR + CB + PV), between ASD cases and matched controls. An adjacent cresyl-violet stained section was used to confirm that the counting frames were located within the boundaries of the desired Brodmann Area using von Economo cytoarchitecture.

Clinical data

We acquired available clinical records for all cases and extracted and coded data regarding ASD symptom severity and comorbidities (see Tables I and S1). For ASD cases, this included autism diagnostic interview—revised (ADI-R) scores, IQ scores, indications of comorbid diagnoses, and autopsy/pathology report information. We classified ASD cases with clinical data indicative of clear intellectual disability (ID clinical diagnosis, or evidence

of full-scale IQ (FSIQ) < 70) as ASD + ID. ADI-R scores were used to determine and classify verbal ability in ASD cases, defined as a functional use of spontaneous language on a daily basis that involves at a minimum use of three-word phrases that are comprehensible to others. All cases classified as control by the NIH NBB and ATP were screened at intake to ensure that such cases were neurologically normal, without any evidence of brain injury, brain disease, or psychiatric illness. Accordingly, we classified all control cases in this study as being without intellectual disability, without epilepsy, and having a verbal ability.

The ADI-R is the standard psychometric instrument used clinically to diagnose autism and consists of 93 questions that characterize the presence and severity of individual ASD symptoms. These questions fall into specific categories and subcategories (Table SI), which reflect abnormalities in reciprocal social interaction (category A), abnormalities in communication (category B), and the presence of restricted, repetitive, and stereotyped patterns of behavior (category C). Increased scores reflect increased symptom severity. An algorithm is utilized to determine if individuals meet a minimum threshold of symptom severity across domains—and if these thresholds are reached, then a diagnosis of autism is made clinically (or confirmed for postmortem cases). Algorithm-transformed scores are used for diagnostic purposes but treat moderate and severe symptomology equivalently. Accordingly, here we utilized untransformed ADI-R scores for assessing correlations between the severity of ASD symptoms and pathology and recalculated Category and Subcategory scores using the same constituent questions.

Statistics

We performed statistical analyses in JMP 16.0.0 (SAS Institute, Cary, NC, USA). We used repeated-measures analysis of variance (ANOVA) to assess differences in IN and cartridge numbers between comorbidity subgroups, and preplanned post hoc contrasts to assess statistical differences between subgroups. *F*-tests were used for both fixed effects and contrasts. Means and standard error of the means are reported. We used Pearson's correlation to assess the relationship between the severity of ASD pathology with the severity of ASD symptomology, as indicated by each case's ADI-R scores, and nonparametric Spearman's rank correlations to assess the relationship between the severities of interneuron pathology with case IQ. For all analyses, $\alpha = 0.05$. As this was an exploratory study using a scarce resource (human postmortem brain tissue from ASD cases), we did not adjust alpha for multiple comparisons to avoid excessive type II error.

Results

We set out to understand the relationship between pathological alterations in IN anatomy with ASD with clinical symptoms. To do so, we used two previously published data sets generated in our laboratory from which we discovered a reduction in the number of PV^+ ChCs in the human ASD prefrontal cortex (Amina et al., 2021; Hashemi et al., 2017). Human postmortem ASD and control brain tissue was acquired from the NIH Neurobiobank (NBB) and the Autism Tissue Program (ATP) for both studies. This included fixed samples from the prefrontal cortex, including the dorsolateral prefrontal (DLPFC: BA9, BA46) and orbitofrontal (OFC, BA47) cortices (Figure 1A). The first experiment (Hashemi et al.,

2017) utilized triple enzymatic immunohistochemistry to label CB-, CR-, and PV-expressing interneurons within single sections for all cases (Figure 1C). This dataset included 11 ADI-R confirmed ASD cases (11M/0F, age: 26.5 ± 4.5 years, PMI: 25.9 ± 8.6 h, brain mass: 1492.5 ± 54.1 g) and 9 matched controls (8M/1 F, age: 35.1 ± 4.6 years, PMI: 25.8 ± 1.8 h, brain mass: 1491.0 ± 67.1 g). There were no significant differences in age, PMI, or brain mass ($p > 0.05$ for all). A subset of ASD cases in this cohort had the following comorbidities: intellectual disability ($n = 5/11$), non verbal ($n = 5/11$), and epilepsy ($n = 2/11$). For each Brodmann area, all CR, CB, and PV $^{+}$ INs were quantified within a 3-mm-wide counting frame that spanned all cortical layers. To obviate the potential confounds of tissue shrinkage and/or poor tissue quality, we utilized the ratios of each IN subtype to the total neurons for statistical analysis and retained the raw cell count data for each case that was also used here. We found significant reductions in the ratio of PV^{+} INs to other INs in ASD, relative to controls—including a 45% reduction in BA9 ($p = 0.030$), 70% in BA46 ($p = 0.001$), and 38% in BA47 ($p = 0.030$). The second experimental dataset comes from a study where we assessed changes in GABA transporter 1 (GAT1) positive cartridges, GABAergic terminals that are anatomically distinct and specific to PV^{+} ChCs (Figure 1B and C). This dataset included 11 ADI-R confirmed ASD cases (11M/0F, age: 15.3 ± 1.6 years, PMI: 15.7 ± 3.9 h, brain mass: 1455.1 ± 43.1 g) and 11 matched controls (7M/4F, age: 15.7 ± 1.6 years, PMI: 21.6 ± 3.1 h, brain mass: 1376.4 ± 36.7 g). There were no significant differences in age, PMI, or brain mass ($p > 0.05$ for all). A subset of ASD cases in this cohort had the following comorbidities: intellectual disability ($n = 7/11$), non verbal ($n = 6/11$), and epilepsy ($n = 4/11$). For each Brodmann area, all $GAT1^{+}$ cartridges were quantified within a 3-mm-wide counting frame that spanned all cortical layers. We found significant reductions in the $GAT1^{+}$ cartridges in ASD, relative to control cases—including a 39% reduction in BA9 ($p = 0.002$), 61% in BA46 ($p = 0.004$), and 46% in BA47 ($p = 0.020$). Together, these datasets illustrate a significant reduction in ChCs in ASD, using two separate markers and using two separate case cohorts (with the exception of 2 ASD and 1 control case that were used in both experiments). Detailed case data are outlined in Table I.

For the current study, we obtained extensive clinical records from the cases included in the previous studies and extracted symptom severity and comorbidity data from each case using postmortem ADI-R scores and clinical histories. We took advantage of the fact that there is tremendous patient heterogeneity in symptom profile, and thus assessed whether variation in ASD symptom severity corresponded with previously quantified variation in IN anatomy. More specifically, we assessed the relationship between IN pathology (reductions in the total number of total and specific INs, PV^{+} neuron ratio, and number of $GAT1^{+}$ cartridges) with ASD symptomology (ADI-R scores and subscores, IQ scores, and comorbidities) in the three prefrontal areas of interest using ANOVA and correlation analysis. Herein, we described positive findings.

Total interneuron number is reduced in ASD cases with intellectual disability

We first assessed whether the severity and/or pattern of interneuron pathology was associated with specific ASD comorbidities. We found a striking difference in the pattern of total IN loss (CR + CB + PV) that corresponded with intellectual disability (Figure 2). Analysis with repeated-measures ANOVA revealed that the total number of INs was

significantly reduced (Group: $p = 0.025$) in ASD cases with ID (ASD + ID, MEAN ± SEM: 208.5 ± 37.1 INs/bin) by 36.6% relative to ASD cases without ID (ASD, 329.0 ± 31.5 INs/bin, $p = 0.024$) and by 37.0% relative to control cases (340.1 ± 25.7 INs/bin, $p = 0.009$) (Figure 2A). The total IN number was not different between control and ASD cases without ID ($p = 0.788$). There was not a fixed effect of the region ($p = 0.266$) nor was there a group-by-region interaction ($p = 0.890$), suggesting that this reduction in total IN number in ASD + ID reflects a global change across the PFC (Figure 2B).

Accounting for ID in the ASD cohort revealed differences in CR and CB (Figure 2C) neuron populations. ASD cases with ID had 37.1% fewer CB $^{+}$ neurons (59.21 ± 12.5 CB^+ INs/bin, $p = 0.049$) and 27.8% fewer CR^+ neurons (116.4 ± 16.4 CR $^{+}$ INs/bin, Trend: $p = 0.052$) relative to ASD cases without ID (94.1 ± 10.8 CB^+ INs/bin, 161.1 ± 13.8 CR^+ INs/bin). Neither ASD subgroup was significantly different ($p > 0.10$ for both) from control cases (148.0.4 ± 11.3 CR^+ INs/bin, 71.4 ± 8.8 CB^+ INs/bin) with respect to CR^+ or CB^+ IN number. However, while mean CR^+ number was similar between control and ASD cases without ID (nonsignificant 8% elevation, $p = 0.473$), there was a sizable yet nonsignificant ($p = 0.122$) 31.9% elevation in CB^+ INs in ASD without ID. Although not detected statistically here, it is possible that increases CB^+ INs in ASD without ID offset the loss of PV^+ INs in this group (see below), leading to total IN counts that are not different from neurotypical controls.

Consistent with our previous findings across ASD cases, there was a large and significant 38.9% reduction in PV^+ interneurons in ASD without ID (73.8 ± 15.8 PV^+ INs/bin), and even larger 71.4% reduction in ASD + ID (34.6 ± 18.5 PV^+ INs/bin, $p = 0.001$), relative to control cases (120.8 ± 12.9 PV^+ INs/bin) (Figure 2(c)). While there was a large 53.2% reduction in PV $^{+}$ number in ASD + ID relative to ASD without ID, this did not reach statistical significance ($p = 0.124$). However, together these data suggest that ASD + ID cases show more severe IN loss across subtypes, leading to a total reduction in IN number.

Total IN number reduction and CR^+ neuron number reduction are correlated with decreases in IQ

Full-scale IQ (FSIQ) scores were available for five cases from the triple stain cohort and the relationship between FSIQ and IN number (mean count across BA9, BA46, and BA47) was assessed using Spearman's rank Correlations (Figure 2D). ASD cases showed a significant stepwise reduction in total IN number and in CR^+ neuron number that correlated with reductions in FSIQ (rho = 0.90, $p = 0.034$ for both). While similar patterns were found for both CB and PV, these were not statistically significant ($p > 0.10$ for both).

Other ASD comorbidities not associated with differences in or cartridge number

Epilepsy was not associated with further alterations in cartridge number in ASD cases across PFC regions ($p > 0.10$, Figure S1A). Too few ASD cases had comorbid epilepsy ($n = 2$) to assess alterations in the triple stain (IN) cohort. We did find a further 31.7% reduction in BA9 cartridge number (Figure S1B) in ASD cases with ID relative to those without; however, this difference did not reach statistical significance ($p = 0.183$). We did not find any difference between verbal and nonverbal ASD cases with respect to total or individual

(CR/CB/PV) IN number, or cartridge number across all three BA regions ($p > 0.10$ for all analyses).

BA47 ChC pathology is correlated with restricted repetitive behaviors

We next assessed the relationship between the severity of ChC pathology (using PV ratios and cartridge number) with the severity of ASD symptomology as reflected by patient ADI-R category scores in the domains of social behavior (category A), non verbal language (category B), and restricted repetitive behaviors (category C, RRB). ADI-R correlations are summarized in Table 2. Specific correlations of interest are highlighted in Figure 3.

Restricted repetitive behavior category scores (C) were strongly correlated with the severity of ChC pathology in BA47 (Figure 3A, $r = -0.822$, $p = 0.012$), with RRB symptom severity increasing in tandem with increasing ChC pathological severity (decreasing PV ratios). There was not a relationship between PV ratios and RRB category scores in either BA9 or BA46 ($p > 0.10$ for both). Cartridge number did not show a significant relationship with the RRB category score in any region in our second ASD cohort (Figure 3 and Table 2, $p > 0.10$ for all).

ADI-R category score C reflects the severity of RRBs across multiple subcategories, including circumscribed Interests (C1), compulsive routines or rituals (C2), stereotypic motor mannerisms (C3), and a preoccupation with parts of objects and/or materials (C4). We found a specific correlation between the severity of ChC pathology (PV ratio) with the severity of stereotypic motor mannerisms (C3) in BA47 (Figure 3A and (B), $r = -0.722$, $p = .043$). This finding was replicated in the $GAT1^+$ cartridge cohort, with cartridge loss severity also corresponding to an increase in stereotypic motor mannerism severity in BA47 (Figure 3C) and D, $r = -0.710$, $p = 0.049$). We did not detect a relationship between ChC pathology (PV or cartridges) with the other RRB subscores (Figure 3, C1, C2, C4, $p > 0.10$ for all). We did not find a relationship between BA9 and BA46 ChC pathologies with RRB subscores (Table 2, $p > 0.10$).

Ch pathology is marginally correlated with nonverbal social-communication deficits

We did not find any significant correlations between ChC pathology (PV ratios or cartridge number) with ASD social deficits in any brain region, with respect to total category score (A), or any category subscores ($p > 0.10$). However, we found a trending relationship between the severity of cartridge loss with the severity of nonverbal communication deficits. The total nonverbal language deficit severity (Category B—nonverbal) increased as BA9 cartridge number decreased (Figure S2, $r = -0.652$, $p = 0.057$), illustrating that increased ChC pathological severity in BA9 is associated with increased social-communication deficits. This correlation was not associated with cartridge loss in BA46 or BA47 ($p > 0.10$). The nonverbal category B score is a composite of subcategory B1 (lack/delay in spoken language and gestures) and B4 (lack of spontaneous play). There was a trending correlation between B4 and cartridge number (Figure S2, $r = -0.660$, $p = 0.053$), but the B1 score was not statistically associated with cartridge pathology (Figure S2, $r = -0.448$, $p = 0.227$).

Discussion

We identified that distinct patterns of GABAergic interneuron pathology in the ASD prefrontal cortex correspond with specific ASD symptoms. ASD cases with intellectual disability show a more widespread and severe pattern of IN loss, while those without ID only show a specific loss in PV^+ INs. Increased severity of ASD motor stereotypies was significantly correlated with increased levels of ChC pathology in BA47, as indicated by reductions in PV^+ neurons and $GAT1^+$ cartridges. We also found a trending correlation between a lack of spontaneous play and an indicator of social communication, with cartridge loss in BA9. We did not detect any link between ChC pathology and other types of restricted repetitive behaviors nor with ASD core social deficits or comorbid epilepsy.

Motor stereotypies, defined as motor patterns that are repetitive, invariant, and seemingly functionless (American Psychiatric Association, 2013; M. Lewis & Kim, 2009; Mason, 1991), are a common behavioral symptom present in numerous neurodevelopmental and psychiatric disorders (American Psychiatric Association, 2013; Kataoka et al., 2010; M. Lewis & Kim, 2009; Morrens et al., 2006), including ASD (Yerys, 2015). They are believed to represent failures in behavioral inhibition, and abnormalities in corticostriatal circuit function have long been theorized to underlie such phenomena (Albin et al., 1995; M. Lewis & Kim, 2009; Yerys, 2015). Corticostriatal circuits are responsible for selecting/activating particular behavioral sequences (striatal direct pathway) or terminating/inhibiting behavioral sequences (striatal indirect pathway) (Albin et al., 1995). These circuits run in five discrete parallel pathways, consisting of closed loops running from the cortex to basal ganglia to the thalamus and back to the cortex (Albin et al., 1995; Alexander et al., 1986). Each of the five pathways represents connections to different cortical regions including the anterior cingulate (ACC), orbitofrontal (OFC), dorsolateral prefrontal (DLPFC), motor (M), and oculomotor (OM) (Alexander et al., 1986)—which are believed to correspond with different levels of behavioral selection, from motivation (limbic loop: ACC/OFC), to cognition (associative loop: DLPFC), to specific motor sequences and individual movements (motor/oculomotor loops: M/OM) (Albin et al., 1995; Garner et al., 2011; Yerys, 2015). Here, we identified a specific putative circuit-level mechanism by which corticostriatal circuits may be disinhibited in BA47 and thus pathologically contribute to ST stereotypies in a complex human disorder—a failure of ChC inhibition of pyramidal neurons, which exclusively mediate information flow from the cortex to the striatum, leads to behavioral disinhibition. If this hypothetical mechanism is true, we would expect that a loss of ChC input into layer V pyramidal cells, the main output from the cortex to the striatum, would be the main driver of such a circuit-level deficit. It is hypothesized that an imbalance in direct/indirect corticostriatal circuitry may be responsible for perseverative behavior at the level of the striatum—specifically that there is an excessive activity in the striatal direct pathway (increased/inappropriate behavioral selection/activation) and/or a deficit in the striatal indirect pathway (reduced/failure of behavioral inhibition) (Garner et al., 2011; M. Lewis & Kim, 2009). Although speculative, cortical pyramidal cell disinhibition would presumably be associated with an abnormal increase in activity of both downstream striatal direct and indirect pathways. Consistent with this, stereotypic behavior is associated with increased functional connectivity between dorsal attention and subcortical networks

(McKinnon et al., 2019). However, it is not clear how pyramidal cell disinhibition, mediated by ChC loss, could result exclusively in attenuated indirect pathway activity and associated disinhibition. Future work with *in vivo* models will be necessary to elucidate how ChC loss in the prefrontal cortex will differentially affect direct and indirect pathway circuits, and how such alterations would manifest behaviorally. It is important to also acknowledge that it is possible, if not likely, that superficial layer (i.e. layer II/III pyramidal cells) cortical-cortical circuits are also disinhibited due to ChC losses in ASD. However, the mechanism by which disinhibited intraregional and intrahemispheric cortical-cortical signaling could contribute to this class of behavioral symptoms in ASD is unclear.

ASD stereotypies were correlated specifically with ChC pathology in the OFC (BA47) but not in the DLPFC (BA9 and BA47). This was surprising, as most corticostriatal dysfunction hypotheses of ST predict that disinhibition in the motor or associative loops (DLPFC), or their corresponding striatal targets, drive this type of repetitive behavior (Garner et al., 2011; M. Lewis & Kim, 2009). OFC hyperactivity is strongly implicated in the pathophysiology of obsessive-compulsive disorder (OCD) (Saxena et al., 1998), a psychiatric illness characterized by unusual anxiety-driven obsessions which in turn drive ritualized compulsive behaviors (American Psychiatric Association, 2013). For this reason, OFC dysfunction is believed to contribute to higher-order repetitive behaviors (i.e. obsessions and/or compulsions), but not stereotypes. Nevertheless, our findings are consistent with fMRI and MR-spectroscopy literature. ASD cases show increased OFC activity during motor inhibition tasks (Schmitz et al., 2006). In addition, reduced cortical GABA levels in the ACC and striatum, but not the DLPFC or premotor cortices, correlate with the severity of motor stereotypies in nonautistic individuals with stereotypic movement disorder (Harris et al., 2016). PV^+ INs are present throughout the cortex as well as most subcortical structures, including the striatum. PV^+ IN alterations have been discovered in other psychiatric disorders, suggesting that their loss may play a role in repetitive behaviors more broadly. Striatal PV^+ INs are reduced in Tourette syndrome (Kataoka et al., 2010), a disorder characterized by both complex and simple repetitive behaviors (i.e. tics), including stereotypies. PV^+ ChCs are also impaired in schizophrenia (D. A. Lewis, 2011), a disorder in which altered motor activity (American Psychiatric Association, 2013) and stereotypies (Morrens et al., 2006) are common. Although the integrity of ChCs in human OCD is uncharacterized, patients show regional hyperactivity (as indicated by fMRI) (Adler et al., 2000) and GABAergic deficits (Zhang et al., 2016) in the OFC. It remains a possibility that a loss of OFC ChCs or other INs may be involved in OCD. Moving forward, it will be important to characterize PV^+ loss in brain regions outside of the PFC in ASD, particularly the striatum, and to assess their involvement in other ASD symptoms.

While large-scale developmental disruptions in brain organization are believed to broadly underlie the complex cognitive deficits that constitute ID, specific circuit-level mechanisms are poorly understood. ID is a symptom that occurs in many disorders of differing etiologies, including approximately 33% of ASD cases (Maenner et al., 2020). Of the numerous genetic and environmental causes of ID, the two most prevalent are Trisomy 21 (Down syndrome (DS)) and fetal exposure to ethanol (fetal alcohol syndrome (FAS)) (Pulsifer, 1996). Neuropathological alterations in the brain structure have been identified for both, and key features are reduction in brain mass and neuron counts in DS (Wisniewski, 1990)

and FAS (Roebuck et al., 1998), and reduced dendritic spine density and maturity in DS (Takashima et al., 1994) and FAS (Ferrer & Galofre, 1987). Both of these deficits are also found in idiopathic ID (Purpura, 1974), yet they differ from ASD neuropathology, which typically includes increased cortical neuron number (Courchesne et al., 2011), and as increased dendritic spine density (Hutsler & Zhang, 2010). Increased spine density also occurs in fragile X Syndrome, the most prevalent monogenic cause of ID. Reduced IQ in ASD is correlated with the most extreme increases in spine density (Hutsler & Zhang, 2010) and alterations (increases or decreases) in brain size (Amaral et al., 2017; Miles et al., 2000). While it is possible that these differences in neuropathology simply reflect differences in cognitive deficits that are specific to each ID-associated disorder, it is possible that other neuropathological mechanisms may more specifically and consistently contribute to cognitive impairment in ID. Deficits in GABAergic signaling, possibly involving alterations in GABAergic interneuron populations, is one candidate mechanism that has received interest in recent years (reviewed extensively by Contestabile et al., 2017). A critical recent study identified that GABAergic interneuron proliferation and migration are broadly impaired in human fetuses prenatally exposed to ethanol (Marguet et al., 2020). Another recent study demonstrated that DS-derived iPSCs show a reduction in GABAergic interneuron proliferation/differentiation in vitro and migration when grafted in-vivo resulting in specific a reduction in total CR $^{+}$ interneurons (Huo et al., 2018).

Here, we found for the first time a link between alterations in IN anatomy with intellectual disability in the human postmortem autistic brain, thus providing further support for a GABAergic hypothesis of ID. ASD cases with intellectual disability (ASD + ID) show a clear reduction in total interneuron number (CR + CB + PV) relative to both neurotypical controls and ASD cases without ID. This pattern is consistent within our PFC regions of interest, but it remains unknown if this pattern extends to other cortical and subcortical regions. Our data indicate that a loss of CR^{+} INs and a more severe loss of PV^{+} INs may be a significant contributor to the total IN reduction in ASD + ID. Although ID was not accounted for, reduced CR^{+} density also was recently identified in the human ASD caudate (Adorjan et al., 2017), also consistent with our findings. A dramatic expansion of CR^{+} INs occurred during human cortical evolution, and this change is hypothesized to enable more complex cognitive abilities specific to the human lineage (Dzaja et al., 2014). Our finding of reduced CR^{+} INs in ASD + ID provides further support for this hypothesis, which is also consistent with deficits in CR^{+} IN proliferation and migration identified in DS and FAS (Huo et al., 2018; Marguet et al., 2020). We also found a significant increase in CB^{+} IN counts ASD without ID relative to ASD + ID, and a nonsignificant increase relative to controls. This possibly reflects an increase in CB^{+} INs in ASD without ID, which offsets the loss of PV^{+} INs, resulting in a normalization of total IN counts to control levels.

It remains unclear what causes alterations in ASD IN anatomy. These alterations most likely reflect developmental impairments in proliferation, differentiation, and/or migration of INs. Cortical INs are not generated from radial glia within the neocortex, but instead are generated from neural precursor cells in the ganglionic eminences (Marin & Rubenstein, 2001). While disruptions in these processes cannot be directly assessed in the prenatal human ASD brain, there is abundant indirect evidence consistent with this perspective. Increased neuron number (Courchesne et al., 2011; Falcone et al., 2021) is a well-

established anatomical abnormality in ASD—clearly implicating dysregulation of fetal neurogenesis. Focal dysplasia and heterotopias are common in ASD and reflect errors in neuronal migration (Wegiel et al., 2010). Many prevalent ASD risk genes (e.g. CHD8 (Xu et al., 2018), FMR1 (Wu et al., 2019), Pten (Chen et al., 2015), Shank3 (Zhao et al., 2017)) are also potent regulators of neuron proliferation, differentiation, and migration —suggesting that allele variants in these genes may impair normal neurodevelopmental regulatory controls (Packer, 2016; Xu et al., 2018). Unlike ASD, DS and fetal exposure to ethanol can be identified prenatally; fetal brain tissue from these cases has been used to identify deficits in IN proliferation and migration (Huo et al., 2018; Marguet et al., 2020). Together, these data are highly suggestive that anatomical and circuit-level brain disruptions in ASD reflect abnormalities in neuron proliferation, differentiation, and/or migration. Alternatively, it is possible that early brain development is normal for most ASD cases, and that PV^+ INs do not survive through subsequent developmental stages after the cells are established, either late prenatally or postnatally. In rodents, PV^+ INs are pruned during early postnatal brain development (~30% reduction from PND 5–10), which is regulated by pyramidal cells in an activity-dependent manner (Denaxa et al., 2018; Wong et al., 2018). PTEN, a gene implicated in ASD risk (Butler et al., 2005), is a critical intermediary in this process (Wong et al., 2018). It is possible that ChC loss in ASD occurs as a result of excessive pruning through this experience-dependent mechanism. Autoimmune-driven loss of specific neuronal populations is another potential mechanism for the etiology of various behavioral/psychiatric disorders, particularly childhood-onset disorders involving repetitive behaviors (Kiessling et al., 1994), but is poorly substantiated and highly controversial (Wilbur et al., 2019) (e.g. PANDAS (Swedo et al., 1998) and PANS (Swedo et al., 2012) hypotheses of Tourette syndrome and other childhood-onset repetitive behaviors (Hsu et al., 2021)). Narcolepsy is one of the few substantiated examples of this possible mechanism, whereby an autoimmune-driven loss of $orexin^+$ neurons in the lateral hypothalamus leads to deficits in sleep-wake cycle regulation (Luo et al., 2018; Mahlios et al., 2013). Immune system abnormalities occur in ASD (Guastella et al., 2015; Warren et al., 1986), including maternal autoimmune processes targeting neuronal proteins in the fetal brain (Braunschweig et al., 2013; Martinez-Cerdeno et al., 2016), and thus autoimmunity could theoretically be a mechanism by which PV^+ INs are lost in ASD. PV^+ INs are also particularly vulnerable to stress—as fast-spiking interneurons, they have high metabolic demand and high levels of calcium signaling, both of which render these cells vulnerable to excitotoxic cell death (Reviewed in Ruden et al., 2021). Finally, another possible explanation for altered IN counts in ASD is that this simply reflects transcriptional changes in specific IN markers (i.e. there is a transcriptional reduction in PV mRNA and protein in ASD, leading to the detection of fewer positive cells with IHC), but not an actual reduction in cell number. This is plausible, as PV^+ basket cells undergo experience-dependent changes in PV expression (Donato et al., 2013, 2015), with associated variations in immunofluorescence signal intensity. However, there is no evidence that PV expression is ever fully silenced in PV^+ basket cells, nor is there any evidence that this type of variable PV expression occurs in ChCs. Our previous findings of ChC loss in ASD were detected using two independent markers (PV^+ soma and $GAT1^+$ cartridges) and quantifying different structures (soma vs cartridges), and we found roughly the same magnitude of ChC loss regardless of the method used. For these reasons, we believe that transcriptional alterations in PV are an unlikely explanation for the

reduced number of ChCs detected in the ASD PFC. Nevertheless, this possibility still needs to be ruled out directly, possibly through developmental studies in rodent models or using single-cell molecular analyses in human brain tissue.

Although designed as a retrospective exploratory study, the main limitation of our study is the relatively small sample size, which is common for neuropathological studies due to the scarcity of resource. Balancing statistical analysis to avoid both Type I and Type II error becomes a particular challenge, and most findings here would not hold up to alpha adjustment for post hoc comparisons. While these findings should be considered preliminary and require further validation, we were able to replicate our key findings internally, which provides us with more confidence in their replicability. Our data sets predominantly relied on young male ASD subjects (only one female was included), and thus it is unclear how alterations in INs, ChCs, or their clinical correlates may possibly differ according to sex or age. Regretfully, the cohorts utilized here were constrained by the sample selection in previous studies.

It is poorly understood how specific circuit-level neuropathology maps onto ASD symptomology. Our data provide evidence directly from human cases that IN pathology is an important contributor to ASD symptomology—that ChC loss is involved in RRB symptomology, and that ASD cases with ID show more severe IN loss, which suggests a similar but more severe developmental insult is occurring in these individuals. These anatomical alterations most likely reflect developmental impairments in proliferation, migration, and/or survival of INs. Our findings identify novel testable hypotheses concerning how alterations in INs may disrupt neural circuits. It also identifies IN pathology as an important biomarker for ASD animal model validation, for ASD developmental studies, and for developing targeted therapeutics that are thus far lacking for ASD patients. 2

Supplementary Material

Refer to Web version on PubMed Central for supplementary material.

Acknowledgements

This work was supported by grants from the National Institute of Mental Health (NIMH) R01MH094681, Medical Investigation of Neurodevelopmental Disorders (MIND) Institute (IDDRC; U54HD079125), Shriners Hospitals, and the Autism Postdoctoral Research Training Program (5T32MH073124-18, BD). We thank Autism BrainNet, sponsored by the Simons Foundation, and its predecessor the Autism Tissue Program, funded by Autism Speaks, for the tissue and the associate clinical data. We also thank the NIH NeuroBioBank.

Thanks to Ezzat Hashemi and Sarwat Amina for generating the neuropathology data sets, including interneuron cell counts and cartridge counts. Special thanks to Carolyn Hare, clinical Director of Autism BrainNet, who conducted the ADI-R interviews for the ATP cases and provided raw (untransformed) ADI-R scores and other clinical records. Thanks to Alexandra LeFevre from the University of Maryland Brian Bank for providing ADI-R scores and clinical records for all NIH NBB cases used here. Thanks also to David Amaral (MIND Institute) for helping to resolve hemi-sphere identification for ATP cases, and to Blythe Durbin-Johnson (MIND Institute) for statistical guidance and suggestions.

Funding

The author(s) disclosed receipt of the following financial support for the research, authorship, and/or publication of this article: VMC—NIMH MH094681; Shriners Hospitals; BD—NIH/MIND Institute Autism Training Research Program T32 (5532MH073124-18).

Availability of data and materials

Please contact author for data requests.

References

Adler CM, McDonough-Ryan P, Sax KW, Holland SK, Arndt S, & Strakowski SM (2000). fMRI of neuronal activation with symptom provocation in unmedicated patients with obsessive compulsive disorder. Journal of Psychiatric Research, 34(4–5), 317–324. 10.1016/s0022-3956(00)00022-4 [PubMed: 11104844]

Adorjan I, Ahmed B, Feher V, Torso M, Krug K, Esiri M, . . . Szele FG (2017). Calretinin interneuron density in the caudate nucleus is lower in autism spectrum disorder. Brain, 140(7), 2028–2040. 10.1093/brain/awx131 [PubMed: 29177493]

Albin RL, Young AB, & Penney JB (1995). The functional anatomy of disorders of the basal ganglia. Trends in Neurosciences, 18(2), 63–64. [PubMed: 7537410]

Alexander GE, DeLong MR, & Strick PL (1986). Parallel organization of functionally segregated circuits linking basal ganglia and cortex. Annual Review of Neuroscience, 9, 357–381. 10.1146/annurev.ne.09.030186.002041

Amaral DG, Li D, Libero L, Solomon M, Van de Water J, Mastergeorge A, . . . Wu Nordahl C. (2017). In pursuit of neurophenotypes: The consequences of having autism and a big brain. Autism Research, 10(5), 711–722. 10.1002/aur.1755 [PubMed: 28239961]

American Psychiatric Association. (2013). Diagnostic and statistical manual of mental disorders (5th ed.). American Psychiatric Publishing.

Amina S, Falcone C, Hong T, Wolf-Ochoa MW, Vakilzadeh G, Allen E, . . . Martinez-Cerdeno V. (2021). Chandelier cartridge density is reduced in the prefrontal cortex in autism. Cerebral Cortex, 31(6), 2944–2951. 10.1093/cercor/bhaa402 [PubMed: 33527113]

Ariza J, Rogers H, Hashemi E, Noctor SC, & Martinez-Cerdeno V.(2018). The number of chandelier and basket cells are differentially decreased in prefrontal cortex in autism. Cerebral Cortex, 28(2), 411–420. 10.1093/cercor/bhw349 [PubMed: 28122807]

Beer JS, John OP, Scabini D, & Knight RT (2006). Orbitofrontal cortex and social behavior: Integrating self-monitoring and emotion-cognition interactions. Journal of Cognitive Neuroscience, 18(6), 871–879. 10.1162/jocn.2006.18.6.871 [PubMed: 16839295]

Braunschweig D, Krakowiak P, Duncanson P, Boyce R, Hansen RL, Ashwood P, . . . Van de Water J.(2013). Autism-specific maternal autoantibodies recognize critical proteins in developing brain. Translational Psychiatry, 3, e277. 10.1038/tp.2013.50 [PubMed: 23838888]

Butler MG, Dasouki MJ, Zhou XP, Talebizadeh Z, Brown M, Takahashi TN, . . . Eng C.(2005). Subset of individuals with autism spectrum disorders and extreme macrocephaly associated with germline PTEN tumour suppressor gene mutations. Journal of Medical Genetics, 42(4), 318–321. 10.1136/jmg.2004.024646 [PubMed: 15805158]

Casanova MF, Buxhoeveden DP, Switala AE, & Roy E.(2002). Minicolumnar pathology in autism. Neurology, 58(3), 428–432. 10.1212/wnl.58.3.428 [PubMed: 11839843]

Chen Y, Huang WC, Sejourne J, Clipperton-Allen AE, & Page DT (2015). Pten mutations alter brain growth trajectory and allocation of cell types through elevated beta-catenin signaling. Journal of Neuroscience, 35(28), 10252–10267. 10.1523/JNEUROSCI.5272-14.2015 [PubMed: 26180201]

Contestabile A, Magara S, & Cancedda L.(2017). The GABAergic hypothesis for cognitive disabilities in down syndrome. Frontiers in Cellular Neuroscience, 11, Article 54. 10.3389/fncel.2017.00054

Courchesne E, Mouton PR, Calhoun ME, Semendeferi K, Ahrens-Barbeau C, Hallet MJ, . . . Pierce K.(2011). Neuron number and size in prefrontal cortex of children with autism. JAMA, 306(18), 2001–2010. 10.1001/jama.2011.1638 [PubMed: 22068992]

DeFelipe J, & Gonzalez-Albo MC (1998). Chandelier cell axons are immunoreactive for GAT-1 in the human neocortex. NeuroReport, 9(3), 467–470. 10.1097/00001756-199802160-00020 [PubMed: 9512391]

DeFelipe J, Lopez-Cruz PL, Benavides-Piccione R, Bielza C, Larranaga P, Anderson S, . . . Ascoli GA (2013). New insights into the classification and nomenclature of cortical GABAergic interneurons. Nature Reviews Neuroscience, 14(3), 202–216. 10.1038/nrn3444 [PubMed: 23385869]

Denaxa M, Neves G, Rabinowitz A, Kemlo S, Liodis P, Burrone J, & Pachnis V.(2018). Modulation of apoptosis controls inhibitory interneuron number in the cortex. Cell Reports, 22(7), 1710–1721. 10.1016/j.celrep.2018.01.064 [PubMed: 29444425]

Donato F, Chowdhury A, Lahr M, & Caroni P.(2015). Early- and late-born parvalbumin basket cell subpopulations exhibiting distinct regulation and roles in learning. Neuron, 85(4), 770–786. 10.1016/j.neuron.2015.01.011 [PubMed: 25695271]

Donato F, Rompani SB, & Caroni P.(2013). Parvalbumin-expressing basket-cell network plasticity induced by experience regulates adult learning. Nature, 504(7479), 272–276. 10.1038/nature12866 [PubMed: 24336286]

Dzaja D, Hladnik A, Bicanic I, Bakovic M, & Petanjek Z.(2014). Neocortical calretinin neurons in primates: Increase in proportion and microcircuitry structure. Frontiers in Neuroanatomy, 8, Article 103. 10.3389/fnana.2014.00103

Falcone C, Mevises NY, Hong T, Dufour B, Chen X, Noctor SC, & Martinez Cerdeno V.(2021). Neuronal and glial cell number is altered in a cortical layer-specific manner in autism. Autism, 25(8), 2238–2253. 10.1177/13623613211014408 [PubMed: 34107793]

Ferrer I, & Galofre E.(1987). Dendritic spine anomalies in fetal alcohol syndrome. Neuropediatrics, 18(3), 161–163. 10.1055/s-2008-1052472 [PubMed: 3683757]

Garner JP, Thogerson CM, Dufour BD, Wurbel H, Murray JD, & Mench JA (2011). Reverse-translational biomarker validation of Abnormal Repetitive Behaviors in mice: An illustration of the 4P's modeling approach. Behavioural Brain Research, 219(2), 189–196. 10.1016/j.bbr.2011.01.002 [PubMed: 21219937]

Guastella AJ, Gray KM, Rinehart NJ, Alvares GA, Tonge BJ, Hickie IB, . . . Einfeld SL (2015). The effects of a course of intranasal oxytocin on social behaviors in youth diagnosed with autism spectrum disorders: A randomized controlled trial. Journal of Child Psychology and Psychiatry, 56(4), 444–452. 10.1111/jcpp.12305 [PubMed: 25087908]

Harris AD, Singer HS, Horska A, Kline T, Ryan M, Edden RA, & Mahone EM (2016). GABA and glutamate in children with primary complex motor stereotypies: An 1H-MRS study at 7T. American Journal of Neuroradiology, 37(3), 552–557. 10.3174/ajnr.A4547 [PubMed: 26542237]

Hashemi E, Ariza J, Rogers H, Noctor SC, & Martinez-Cerdeno V.(2017). The number of parvalbumin-expressing interneurons is decreased in the prefrontal cortex in autism. Cerebral Cortex, 27(3), 1931–1943. 10.1093/cercor/bhw021 [PubMed: 26922658]

Hertrich I, Dietrich S, Blum C, & Ackermann H.(2021). The role of the dorsolateral prefrontal cortex for speech and language processing. Frontiers in Human Neuroscience, 15, Article 645209. 10.3389/fnhum.2021.645209

Hof PR, Glezer II, Conde F, Flagg RA, Rubin MB, Nimchinsky EA, & Vogt Weisenhorn DM (1999). Cellular distribution of the calcium-binding proteins parvalbumin, calbindin, and calretinin in the neocortex of mammals: Phylogenetic and developmental patterns. Journal of Chemical Neuroanatomy, 16(2), 77–116. 10.1016/s0891-0618(98)00065-9 [PubMed: 10223310]

Hsu CJ, Wong LC, & Lee WT (2021). Immunological dysfunction in Tourette syndrome and related disorders. International Journal of Molecular Sciences, 22(2), 853. 10.3390/ijms22020853 [PubMed: 33467014]

Huo HQ, Qu ZY, Yuan F, Ma L, Yao L, Xu M, . . . Liu Y.(2018). Modeling down syndrome with patient iPSCs reveals cellular and migration deficits of GABAergic neurons. Stem Cell Reports, 10(4), 1251–1266. 10.1016/j.stemcr.2018.02.001 [PubMed: 29526735]

Hutsler JJ, & Zhang H.(2010). Increased dendritic spine densities on cortical projection neurons in autism spectrum disorders. Brain Research, 1309, 83–94. 10.1016/j.brainres.2009.09.120 [PubMed: 19896929]

Kataoka Y, Kalanithi PS, Grantz H, Schwartz ML, Saper C, Leckman JF, & Vaccarino FM (2010). Decreased number of parvalbumin and cholinergic interneurons in the striatum of individuals with Tourette syndrome. Journal of Comparative Neurology, 518(3), 277–291. 10.1002/cne.22206 [PubMed: 19941350]

Kiessling LS, Marcotte AC, & Culpepper L.(1994). Antineuronal antibodies: Tics and obsessive-compulsive symptoms. Journal of Developmental and Behavioral Pediatrics, 15(6), 421–425. [PubMed: 7884013]

Kohane IS, McMurry A, Weber G, MacFadden D, Rappaport L, Kunkel L, . . . Churchill S.(2012). The co-morbidity burden of children and young adults with autism spectrum disorders. PLOS ONE, 7(4), Article e33224. 10.1371/journal.pone.0033224

Lawrence YA, Kemper TL, Bauman ML, & Blatt GJ (2010). Parvalbumin-, calbindin-, and calretinin-immuno-reactive hippocampal interneuron density in autism. Acta Neurologica Scandinavica, 121(2), 99–108. 10.1111/j.1600-0404.2009.01234.x [PubMed: 19719810]

Lewis DA (2011). The chandelier neuron in schizophrenia. Developmental Neurobiology, 71(1), 118–127. 10.1002/dneu.20825 [PubMed: 21154915]

Lewis M, & Kim SJ (2009). The pathophysiology of restricted repetitive behavior. Journal of Neurodevelopmental Disorders, 1(2), 114–132. 10.1007/s11689-009-9019-6 [PubMed: 21547711]

Luo G, Ambati A, Lin L, Bonvalet M, Partinen M, Ji X, . . . Mignot EJ (2018). Autoimmunity to hypocretin and molecular mimicry to flu in type 1 narcolepsy. Proceedings of the National Academy of Sciences of the United States of America, 115(52), E12323–E12332. 10.1073/pnas.1818150116 [PubMed: 30541895]

Maenner MJ, Shaw KA, Baio J, Washington A, Patrick M, DiRienzo M, . . .Dietz PM (2020). Prevalence of autism spectrum disorder among children aged 8 years—Autism and developmental disabilities monitoring network, 11 sites, United States, 2016. MMWR Surveillance Summaries, 69(4), 1–12. 10.15585/mmwr.ss6904a1

Mahlios J, De la Herran-Arita AK, & Mignot E.(2013). The autoimmune basis of narcolepsy. Current Opinion in Neurobiology, 23(5), 767–773. 10.1016/j.conb.2013.04.013 [PubMed: 23725858]

Marguet F, Friocourt G, Brosolo M, Sauvestre F, Marcorelles P, Lesueur C, . . . Laquerriere A. (2020). Prenatal alcohol exposure is a leading cause of interneuronopathy in humans. Acta Neuropathologica Communications, 8(1), Article 208. 10.1186/s40478-020-01089-z

Marin O, & Rubenstein JL (2001). A long, remarkable journey: Tangential migration in the telencephalon. Nature Reviews Neuroscience, 2(11), 780–790. 10.1038/35097509 [PubMed: 11715055]

Martinez-Cerdeno V, Camacho J, Fox E, Miller E, Ariza J, Kienzle D, . . .Van de Water J.(2016). Prenatal exposure to autism-specific maternal autoantibodies alters proliferation of cortical neural precursor cells, enlarges brain, and increases neuronal size in adult animals. Cerebral Cortex, 26(1), 374–383. 10.1093/cercor/bhu291 [PubMed: 25535268]

Mason GJ (1991). Stereotypies—A critical-review. Animal Behaviour, 41, 1015–1037. https://doi.org/101016/S0003347205806402

McKinnon CJ, Eggebrecht AT, Todorov A, Wolff JJ, Elison JT, Adams CM, . . . Network I. (2019). Restricted and repetitive behavior and brain functional connectivity in infants at risk for developing autism spectrum disorder. Biological Psychiatry: Cognitive Neuroscience and Neuroimaging, 4(1), 50–61. 10.1016/j.bpsc.2018.09.008 [PubMed: 30446435]

Miles JH, Hadden LL, Takahashi TN, & Hillman RE (2000). Head circumference is an independent clinical finding associated with autism. American Journal of Medical Genetics, 95(4), 339–350. [PubMed: 11186888]

Morrens M, Hulstijn W, Lewi PJ, De Hert M, & Sabbe BG (2006). Stereotypy in schizophrenia. Schizophrenia Research, 84(2–3), 397–404. 10.1016/j.schres.2006.01.024 [PubMed: 16549339]

Packer A.(2016). Neocortical neurogenesis and the etiology of autism spectrum disorder. Neuroscience & Biobehavioral Reviews, 64, 185–195. 10.1016/j.neubiorev.2016.03.002

Pulsifer MB (1996). The neuropsychology of mental retardation. Journal of the International Neuropsychological Society, 2(2), 159–176. 10.1017/s1355617700001016 [PubMed: 9375201]

Purpura DP (1974). Dendritic spine “dysgenesis” and mental retardation. Science, 186(4169), 1126–1128. 10.1126/science.186.4169.1126 [PubMed: 4469701]

Roebuck TM, Mattson SN, & Riley EP (1998). A review of the neuroanatomical findings in children with fetal alcohol syndrome or prenatal exposure to alcohol. Alcoholism: Clinical and Experimental Research, 22(2), 339–344. 10.1111/j.1530-0277.1998.tb03658.x [PubMed: 9581638]

Ruden JB, Dugan LL, & Konradi C.(2021). Parvalbumin interneuron vulnerability and brain disorders. Neuropsychopharmacology, 46(2), 279–287. 10.1038/s41386-020-0778-9 [PubMed: 32722660]

Saxena S, Brody AL, Schwartz JM, & Baxter LR (1998). Neuroimaging and frontal-subcortical circuitry in obsessive-compulsive disorder. The British Journal of Psychiatry, 173, 26–37.

Schmitz N, Rubia K, Daly E, Smith A, Williams S, & Murphy DG (2006). Neural correlates of executive function in autistic spectrum disorders. Biological Psychiatry, 59(1), 7–16. 10.1016/j.biopsych.2005.06.007 [PubMed: 16140278]

Snow PJ (2016). The structural and functional organization of cognition. Frontiers in Human Neuroscience, 10, Article 501. 10.3389/fnhum.2016.00501

Sterponi L, de Kirby K, & Shankey J.(2015). Rethinking language in autism. Autism, 19(5), 517–526. 10.1177/1362361314537125 [PubMed: 24916453]

Swedo SE, Leckman JF, & Rose NR (2012). From research subgroup to clinical syndrome: Modifying the PANDAS criteria to describe PANS (pediatric acute-onset neuropsychiatric syndrome). Pediatrics & Therapeutics, 2(2), 113.

Swedo SE, Leonard HL, Garvey M, Mittleman B, Allen AJ, Perlmutter S, . . . Dubbert BK (1998). Pediatric autoimmune neuropsychiatric disorders associated with streptococcal infections: Clinical description of the first 50 cases. American Journal of Psychiatry, 155(2), 264–271. 10.1176/ajp.155.2.264 [PubMed: 9464208]

Takashima S, Iida K, Mito T, & Arima M.(1994). Dendritic and histochemical development and ageing in patients with Down's syndrome. Journal of Intellectual Disability Research, 38(Pt. 3), 265–273. 10.1111/j.1365-2788.1994.tb00394.x [PubMed: 8061472]

Tanji J, & Hoshi E.(2008). Role of the lateral prefrontal cortex in executive behavioral control. Physiological Reviews, 88(1), 37–57. 10.1152/physrev.00014.2007 [PubMed: 18195082]

Wang Y, Zhang P, & Wyskiel DR (2016). Chandelier cells in functional and dysfunctional neural circuits. Frontiers in Neural Circuits, 10, Article 33. 10.3389/fncir.2016.00033

Warren RP, Margaretten NC, Pace NC, & Foster A.(1986). Immune abnormalities in patients with autism. Journal of Autism and Developmental Disorders, 16(2), 189–197. 10.1007/BF01531729 [PubMed: 2941410]

Wegiel J, Kuchna I, Nowicki K, Imaki H, Wegiel J, Marchi E, . . . Wisniewski T.(2010). The neuropathology of autism: Defects of neurogenesis and neuronal migration, and dysplastic changes. Acta Neuropathologica, 119(6), 755–770. 10.1007/s00401-010-0655-4 [PubMed: 20198484]

Wilbur C, Bitnun A, Kronenberg S, Laxer RM, Levy DM, Logan WJ, . . . Yeh EA (2019). PANDAS/PANS in childhood: Controversies and evidence. Paediatrics & Child Health, 24(2), 85–91. 10.1093/pch/pxy145

Wisniewski KE (1990). Down syndrome children often have brain with maturation delay, retardation of growth, and cortical dysgenesis. American Journal of Medical Genetics, 37, 274–281. 10.1002/ajmg.1320370755

Wong FK,Bercsenyi K,Sreenivasan V,Portales A,Fernandez-Otero M, & Marin O.(2018). Pyramidal cell regulation of interneuron survival sculpts cortical networks. Nature, 557(7707), 668–673. 10.1038/s41586-018-0139-6 [PubMed: 29849154]

Wu C, Zhang X, Chen P, Ruan X, Liu W, Li Y, . . . Peng X.(2019). MicroRNA-129 modulates neuronal migration by targeting Fmr1 in the developing mouse cortex. Cell Death & Disease, 10(4), Article 287. 10.1038/s41419-019-1517-1

Xu Q, Liu YY, Wang X, Tan GH, Li HP, Hulbert SW, . . . Jiang YH (2018). Autism-associated CHD8 deficiency impairs axon development and migration of cortical neurons. Molecular Autism, 9, Article 65. 10.1186/s13229-018-0244-2

Yerys BE (2015). An update on the neurobiology of repetitive behaviors in autism. International Review of Research in Developmental Disabilities, 49, 91–150. 10.1016/bs.irrdd.2015.06.006

Zaitsev AV, Gonzalez-Burgos G, Povysheva NV, Kroner S, Lewis DA, & Krimer LS (2005). Localization of calcium-binding proteins in physiologically and morphologically characterized interneurons of monkey dorsolateral prefrontal cortex. Cerebral Cortex, 15(8), 1178–1186. 10.1093/cercor/bhh218 [PubMed: 15590911]

Zhang Z, Fan Q, Bai Y, Wang Z, Zhang H, & Xiao Z.(2016). Brain gamma-aminobutyric acid (GABA) concentration of the prefrontal lobe in unmedicated patients with obsessive-compulsive disorder: A research of magnetic resonance spectroscopy. Shanghai Archives of Psychiatry, 28(5), 263–270. 10.11919/j.issn.1002-0829.216043 [PubMed: 28638200]

Zhao H, Tu Z, Xu H, Yan S, Yan H, Zheng Y, . . . Zhang YQ. (2017). Altered neurogenesis and disrupted expression of synaptic proteins in prefrontal cortex of SHANK3-deficient non-human primate. Cell Research, 27(10), 1293–1297. 10.1038/cr.2017.95 [PubMed: 28741620]

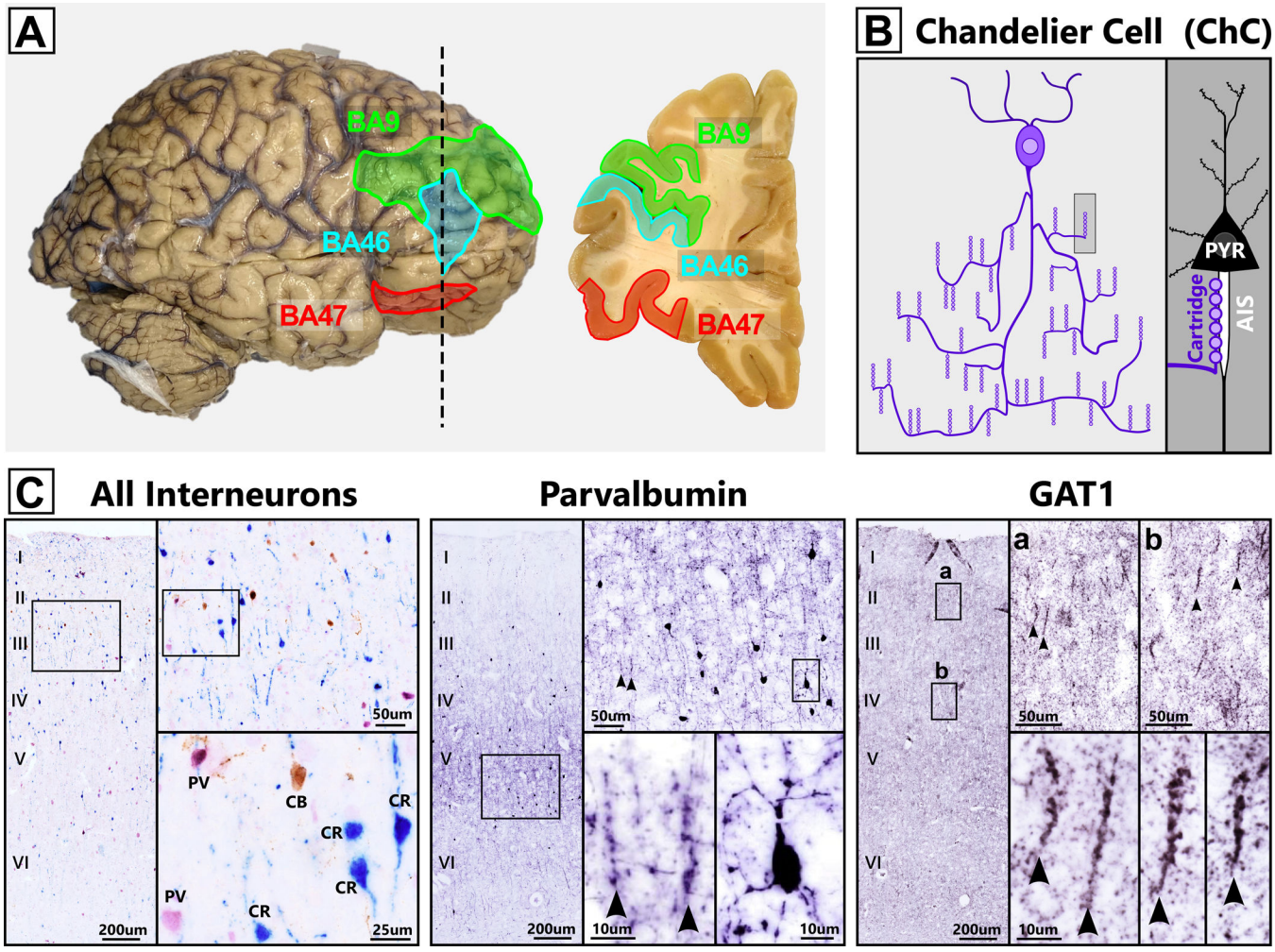

Figure 1.

Overview—human postmortem tissue and staining. (A) Anatomical localization of three regions of interest from the prefrontal cortex (BA9, BA46, and BA47), as overlayed onto an intact human brain hemisphere (left) and a coronal slab (right). (B) Illustration of the Chandelier cell (ChC)—a parvalbumin (PV) expressing GABAergic interneuron subtype that is reduced in number in autism. ChCs have a unique morphology, which includes a complex axonal arbor that terminates in numerous sequences of vertically oriented synaptic terminals (Cartridges) which synapse exclusively on the axon initial segment (AIS) of cortical pyramidal (PYR) neurons. (C) Overview of tissue staining, using representative images from BA46. Left: All GABAergic Interneuron subtypes were identified simultaneously with enzymatic immunohistochemistry (IHC) for the calcium-binding protein markers calretinin (CR, blue), calbindin (CB, brown), and PV (purple), which are expressed by all GABAergic Interneurons in a predominantly nonoverlapping manner. Middle: IHC stain for PV to illustrate cortical layer distribution, as well as the presence of PV^{+} soma and cartridges (red arrows). Right: IHC stain for GABA transporter 1 (GAT1), a marker for GABAergic synaptic terminals. ROIs “a” and “b” are enlarged to show individual $GAT1^{+}$ Cartridges at 40× (top) and 100× (below).

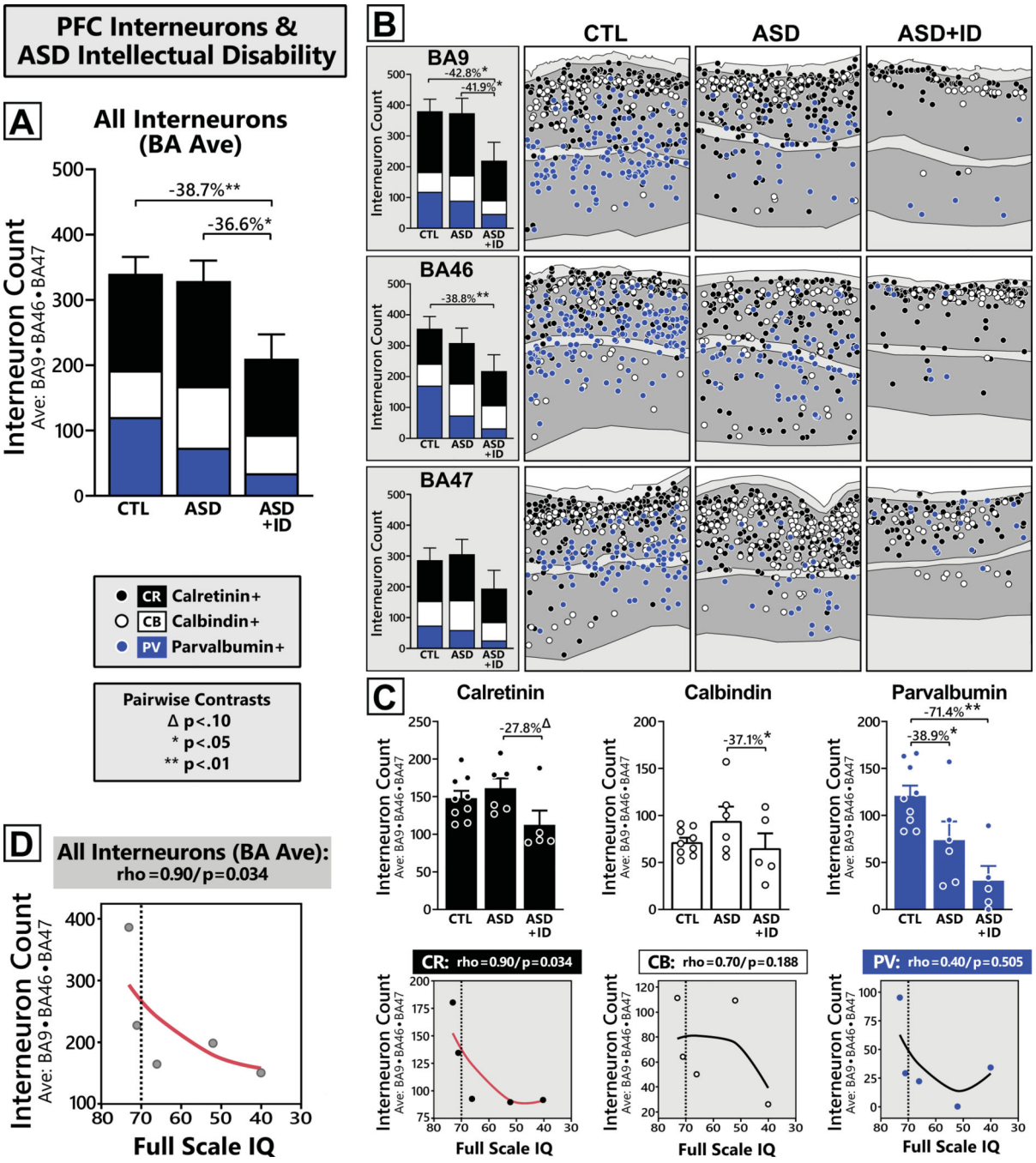

Figure 2.

GABAergic interneuron number and intellectual disability in ASD. (A) Autistic cases with comorbid intellectual disability (ASD + ID) show a significant reduction in total interneuron (IN) number relative to intellectually normal autistic cases (ASD) and neurotypical controls (CTL). Interneuron count reflects the sum of calretinin (CR, black), calbindin (CB, white), and parvalbumin (PV, blue) expressing neurons measured in a 3-mm-wide bin that spanned all cortical layers. There was not a statistical difference between brain regions and brain region-by-group interactions. (B) The same pattern of total IN loss was detected across

all three PFC regions. Reconstructions of IN counts from the three subgroups illustrate a dramatic reduction in total IN number in the ASD + ID group in all three BA regions. (C) ASD + ID showed a 27.8% trending reduction in CR^+ ($p = 0.052$) and a significant 37.1% reduction in CB^+ ($p = 0.049$) INs relative to ASD cases without ID. PV^+ cell number was significantly reduced in both groups of ASD cases relative to controls. (D) Spearman's Rank correlations between Full Scale IQ scores (reverse plot, LOESS curve fit) with total IN counts (left, large), as well as individually for CR, CB, and PV. Although FSIQ was available for only a small subset of cases, all near or below the ID cutoff of FSIQ = 70, reductions in total IN number and CR^+ number were significantly correlated ($p < 0.05$) with reductions in FSIQ. LSM ± SE is shown from repeated-measures ANOVA that included all three cortical regions—BA 9, 46, and 47. For all analyses using ANOVA, pairwise comparisons were made using preplanned post hoc contrasts ($\alpha = 0.05$). Scale bar = 500 μm.

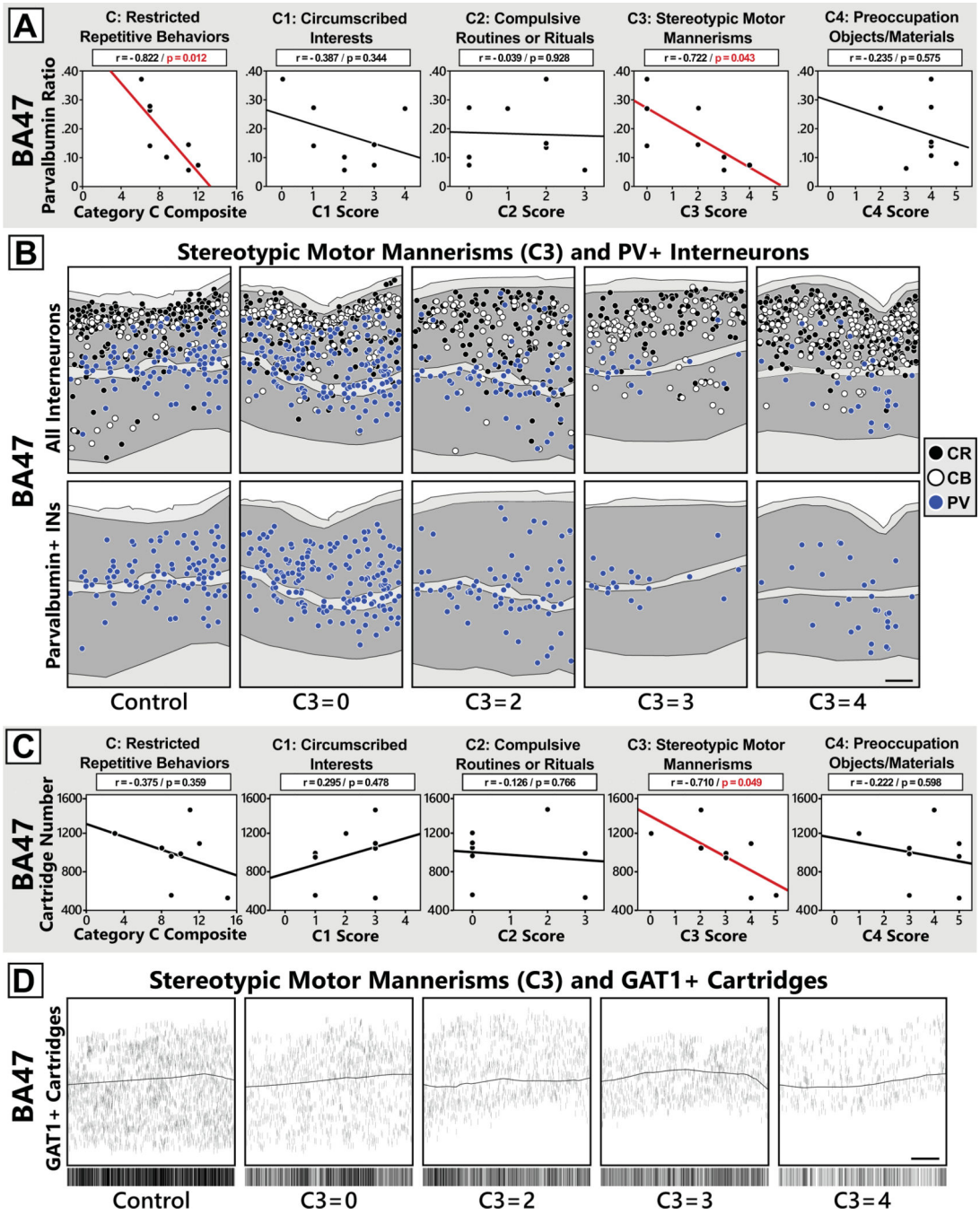

Figure 3.

Chandelier cell loss and ADI-R symptom correlations. Autism core symptom severity, as defined by ADI-R scores, shows a specific relationship with Chandelier Cell (ChC) Pathology, as indicated by reduced PV ratios and cartridges in a region-specific manner. Increased scores reflect increased symptom severity. (A) Reduced PV ratios in the orbitofrontal cortex (OFC, BA47) were correlated with increased severity of Restricted Repetitive Behaviors (Left, ADI-R Category C). Reductions in BA47 PV ratios were significantly ($p < 0.05$) correlated with the severity of stereotypic motor mannerisms (ADI-R

Subcategory C3), but not with other types of RRB such as circumscribed interests (C1), compulsive routines or rituals (C2), or preoccupation with parts of objects or materials (C4). (b) Reconstructions of IN populations (all INs top row, PV^+ INs only bottom row) from individual cases illustrate that a reduced PV^+ Ratio corresponds to increased severity of stereotypic motor mannerisms. (c) Reductions in cartridge number in the orbitofrontal cortex (OFC, BA47) were also correlated with increased severity of stereotypic motor mannerisms (C3), but not with other types of RRB such as circumscribed interests (C1), compulsive routines or rituals (C2), or preoccupation with parts of objects or materials (C4). (d) Reconstructions of cartridge counts (each cartridge is represented by a single vertical line) from individual cases illustrate that a reduced cartridge number corresponds to increased severity of stereotypic motor mannerisms. Linear density of cartridges plotted below reconstruction. Scale bar = 500 μm.

Table I.

Autism and control subjects.

ID	Experiment	Group	Origin	Age	Sex	PMI	brain mass	hemi	Verbal	epilepsy	ID	FULL IQ	Cause of death
AN03221	BOTH	ASD	ATP	7	M	11.4	1560	R	V	NO	NO	UNK	Drowning
ANO 1293	TRIPLE	ASD	ATP	9	M	3.8	1690	L	NV	NO	ID	UNK	Cardiac arrest
AN00394	TRIPLE	ASD	ATP	14	M	10.3	1615	UNK	V	NO	NO	71	Cardiac arrest
AN02736	BOTH	ASD	ATP	15	M	2.5	1390	R	NV	EP	NO	UNK	Aspiration/ pneumonia
AN00764	TRIPLE	ASD	ATP	20	M	23.7	1 144	R	NV	NO	ID	52	Car accident/ trauma
AN00493	TRIPLE	ASD	ATP	27	M	8.3	1575	R	V	NO	ID	40	Drowning
AN 18892	TRIPLE	ASD	ATP	31	M	99	1600	R	V	NO	NO	73	Gun shot
AN0990I	TRIPLE	ASD	ATP	32	M	28.7	1694	R	V	NO	NO	UNK	Heat stress
AN06746	TRIPLE	ASD	ATP	44	M	30.8	1530	UNK	V	NO	ID	66	Cardiac arrest
AN 19534	TRIPLE	ASD	ATP	45	M	40.2	1360	R	NV	EP	NO	UNK	Asphyxiation
AN 18838	TRIPLE	ASD	ATP	48	M	UNK	1260	R	NV	NO	ID	Severe (20–35)	Asphyxiation
5144	Cartridges	ASD	NIH	7	M	3	131 1	R	V	NO	NO	UNK	Cancer
4305	Cartridges	ASD	NIH	12	M	13	1360	R	V	EP	ID	UNK	Serotonin syndrome
AN00754	Cartridges	ASD	ATP	13	M	8.0	1470	R	NV	EP	ID	Mild (50–69)	SUDEP
4899	Cartridges	ASD	NIH	14	M	9	1450	R	NV	EP	NO	UNK	Drowning
5403	Cartridges	ASD	NIH	16	M	35	1777	R	NV	NO	ID	55	Cardiac arhythmia
4269	Cartridges	ASD	NIH	19	M	45	1500	R	V	NO	ID	UNK	Meningitis
4999	Cartridges	ASD	NIH	20	M	14	1427	R	NV	NO	ID	Severe (20–35)	Cardiac arhythmia
5176	Cartridges	ASD	NIH	22	M	18	1525	R	NV	NO	ID	UNK	Subdural hemmorhage
5574	Cartridges	ASD	NIH	23	M	14	1236	R	NV	NO	ID	UNK	Pneumonia
AN07444	BOTH	CTL	ATP	17	M	30.8	1460	R	V	NO	NO	UNK	Asphyxia
AN00544	TRIPLE	CTL	ATP	17	M	28.9	1250	L	V	NO	NO	UNK	UNK
AN 19760	TRIPLE	CTL	ATP	28	M	23.3	1580	R	V	NO	NO	UNK	Cardiac arrest
AN 12137	TRIPLE	CTL	ATP	31	M	32.9	1810	R	V	NO	NO	UNK	Asphyxia
AN 15566	TRIPLE	CTL	ATP	32	F	28.9	1360	R	V	NO	NO	UNK	Heart attack
AN05475	TRIPLE	CTL	ATP	39	M	NK	1350	R	V	NO	NO	UNK	Cardiac arrest
AN 17868	TRIPLE	CTL	ATP	46	M	18.8	1588	R	V	NO	NO	UNK	Cardiac arrest
AN 19442	TRIPLE	CTL	ATP	50	M	20.4	1740	R	V	NO	NO	UNK	Heart attack
AN 13295	TRIPLE	CTL	ATP	56	M	22.1	1370	L	V	NO	NO	UNK	Cardiac arrest
4203	Cartridges	CTL	NIH	7	M	24	1 188	R	V	NO	NO	UNK	Respiratory insufficiency
4337	Cartridges	CTL	NIH	8	M	16	1290	R	V	NO	NO	UNK	Accident
5554	Cartridges	CTL	NIH	13	F	15	1271	R	V	NO	NO	UNK	Suicide
5309	Cartridges	CTL	NIH	14	F	8	UNK	R	V	NO	NO	UNK	Infection

ID	Experiment	Group	Origin	Age	Sex	PMI	brain mass	hemi	Verbal	epilepsy	ID	FULL IQ	Cause of death
5834	Cartridges	CTL	NIH	14	M	38	1510	R	V	NO	NO	UNK	Cardiac failure
4638	Cartridges	CTL	NIH	15	F	5	1250	R	V	NO	NO	UNK	Accident/chest injuries
5893	Cartridges	CTL	NIH	19	M	19	1550	R	V	NO	NO	UNK	Dilated cardiomegaly
5646	Cartridges	CTL	NIH	20	F	23	1440	R	V	NO	NO	UNK	Reactive airway disease
5958	Cartridges	CTL	NIH	22	M	24	1440	R	V	NO	NO	UNK	Dilated cardiomegaly
ANO 1891	Cartridges	CTL	ATP	24	M	35	1365	L	V	NO	NO	UNK	Trauma/car accident

PMI = Post-Mortem Interval (hours)

Triple = triple stained tissue for IN subtype analysis (calretinin, calbindin, parvalbumin). Cartridges = GABA transporter I (GATI) Stained tissue for cartridge counts.

Group: ASD = autism spectrum disorder diagnosis, all confirmed with postmortem ADI-R.

Group: CTL = control subjects.

Origin: ATP = autism tissue program/NIH = NIH Neurobiobank.

Verbal: NV = nonverbal; V = verbal.

EP = Epilepsy co-morbidity present.

ID = intellectual disability (MR/ID clinical diagnosis, or full scale IQ < 70).

Table 2.

ADI-R category and subcategory symptom correlations with Chandelier cell pathology.

	PV ratio						Cartridges					
	BA9 (DLPFC)		BA46 (DLPFC)		BA47 (OFC)		BA9 (DLPFC)		BA46 (DLPFC)		BA47 (OFC)	
	r	*p*	*r*	*p*	*r*	*p*	*r*	*p*	*r*	*p*	*r*	*p*
A. Social deficits	0.029	0.946	0.055	0.889	−0.101	0.811	−0.173	0.711	0.535	0.216	−0.206	0.695
Al Nonverbal social	−0.021	0.961	0.218	0.573	−0.187	0.657	0.056	0.886	0.064	0.870	0.078	0.854
A2 Peer relationships	0.0 15	0.972	−0.232	0.547	0.097	0.819	−0.496	0.211	0.483	0.225	−0.471	0.286
A3 Shared enjoyment	0.367	0.371	0.468	0.204	−0.060	0.888	−0.084	0.830	0.032	0.935	−0.1 17	0.782
A4 Socioemotional reciprocity	−0.103	0.809	−0.091	0.817	−0.177	0.674	−0.024	0.956	0.475	0.235	0.020	0.966
B. Nonverbal language deficits	0.084	0.843	0.231	0.550	−0.048	0.910	−0.652	0.057	0.158	0.684	−0.357	0.386
Bl Spoken language	−0.175	0.678	0.087	0.824	−0.098	0.818	−0.448	0.227	0.294	0.442	−0.246	0.558
B4 Lack of spontaneous play	0.393	0.336	0.343	0.367	0.022	0.960	−0.660	0.053	−0.162	0.678	−0.325	0.433
C. Restricted repetitive behaviors	0.061	0.886	−0.167	0.668	−0.822	0.012	0.174	0.654	−0.118	0.763	0.375	0.359
Cl Circumscribed interests	−0.142	0.737	−0.294	0.443	−0.387	0.344	0.397	0.291	0.442	0.233	0.295	0.478
C2 Compulsive routines/rituals	−0.574	0.137	−0.133	0.733	−0.039	0.928	0.373	0.322	−0.405	0.280	−0.126	0.766
C3 Stereotyped motor	0.348	0.398	−0.160	0.681	**−0.722**	**0.043**	−0.441	0.235	−0.086	0.826	**−0.710**	**0.049**
C4 Preocc. objects/ nonfunct	0.503	0.204	0.518	0.153	−0.235	0.575	0.012	0.976	−0.173	0.656	−0.222	0.598

ADI-R: autism diagnostic interview—revised; DLPFC: dorsolateral prefrontal; OFC: orbitofrontal; PV: parvalbumin. Significant correlations ($p < 0.05$) in bold.